Turbulent Transport with Stochastic Magnetic Field Lines

P Beyer†, S Benkadda†, X Garbet‡, P Ghendrih‡, and Y Sarazin‡

†Equipe Dynamique des Systèmes Complexes, Laboratoire PIIM CNRS – Université de Provence, Marseille, France
‡Association EURATOM – CEA, CEA Cadarache, France

E-mail: beyer@up.univ-mrs.fr

Abstract. Turbulent transport at the edge of a tokamak plasma is strongly affected by magnetic field perturbations induced by an ergodic divertor. Experimental observations show a decrease of density fluctuations and a stabilization of large scale structures. Surprisingly, there is no evidence of a change of the turbulent cross field diffusivity. In the present work, these features are reproduced by 3D numerical simulations of resistive ballooning turbulence driven by a constant heat flux from the plasma core. Additionally, the simulations show an increase of velocity fluctuations in the stochastic region which provides an explanation for the observation of an roughly unchanged mean turbulent flux. This result is important for the performance of the ergodic divertor since any means of lowering the confinement in the divertor volume opens the operational space of the divertor. Although the present analysis is applied to the Tore Supra ergodic divertor, the basic trends of the model and analysis must capture features of transport during ELMs. An important feature of the dynamics of turbulent transport is the appearance of large scale transport events induced by radially elongated convection cells (streamers) and the interplay of the latter with sheared mean and zonal flows. In the stochastic layer, the poloidal mean flow is found to be suppressed and zonal flows are reduced. Larger turbulent fronts propagating in the radial direction tend to resist the shearing induced by the stochasticity of the magnetic field lines.

1. Introduction

The aim of this work is to provide an understanding of basic effects of static magnetic field perturbations on turbulence and transport at the tokamak plasma edge. The interest on this topic is twofold: First, the presence of turbulent cross field transport in regions of stochastic magnetic field lines is highly important for the performance of ergodic divertors [1]. Second, the model of turbulence in the presence of magnetic field perturbations allows to study transport due to the so called magnetic flutter, i.e. the fact that transport *parallel* to the *perturbed* magnetic field can have a significant component *perpendicular* to the *unperturbed* field. This effect is one part of the complete problem of electromagnetic turbulence and transport. Furthermore, the basic trends of the model and analysis must capture features of transport during ELMs insofar that one considers that stochasticity plays a significant role in the onset of transport during ELMs.

Experimental observations of density fluctuations on TEXT [2] and Tore Supra [3, 4, 5] with ergodic divertor show a decrease of the fluctuation level and a stabilization of large scale structures in the stochastic region. Surprisingly, there is no evidence of a change of the turbulent cross field diffusivity [1, 6].

The problem is modeled using 3D numerical simulations of resistive ballooning turbulence including magnetic field perturbations similar to those induced by the divertor coils on Tore Supra. In previous works [7, 8], simulations in a simplified model reproduced qualitatively the experimentally observed decrease of the density fluctuation level as well as the stabilization of large scale structures. Additionally, an increase of the velocity fluctuation level was found which provides an explanation for the experimental observation of a roughly unchanged level of turbulent flux. This result is important for the performance of the ergodic divertor since any means of lowering the confinement in the divertor volume opens the operational space of the divertor. Concerning transport during ELMs, a similar statement can be made, since stochasticity does not quench the anomalous cross-field transport, the latter remains effective in spreading the heat pulse.

In the present work, two important improvements of the model have been made. First, the dynamics of Fourier modes that are not resonant with the magnetic field perturbation are included. Second, the assumption of scale separability between equilibrium and fluctuations has been dropped and the fluctuations are allowed to modify the profiles. Regarding the pressure profile, this allows for the radial propagation of low or high pressure "bursts" [9]. These large scale transport events are linked to radially elongated convection cells ("streamers") [10] which are expected to be strongly affected by the shearing due to stochastic field lines. The dynamics of the poloidal velocity profile is also included self-consistently which allows for the generation of sheared mean and zonal flows by both, the turbulence and the magnetic field perturbation. As the regulation of large scale transport events via these flows plays a significant role in determining the dynamics of turbulent transport [10, 11], the latter is expected to be strongly influenced by the magnetic field perturbation not only due to a change of the fluctuation amplitudes and/or phase but also via a modification of

sheared mean and zonal flows.

2. Model equations

The model consists of normalized reduced electrostatic MHD equations for the electric potential ϕ and the pressure p [7]:

$$d_t \nabla_\perp^2 \phi = -\nabla_\parallel^2 \phi - Gp + \nu \nabla_\perp^4 \phi \ , \tag{1}$$

$$d_t p = \delta_c G\phi + \chi_\parallel \nabla_\parallel^2 p + \chi_\perp \nabla_\perp^2 p + S \ . \tag{2}$$

Here $d_t = \partial_t + \{\phi, \ \cdot \ \}$, where the Poisson bracket represents the convection due to the $\vec{E} \times \vec{B}$ velocity $\vec{v} = \vec{v}_{E\times B}$. The gradients are split into components parallel and perpendicular to the magnetic field which is given by $\vec{B} = B_\varphi \{\hat{e}_\varphi + r/[Rq(r)]\hat{e}_\theta\} + \delta\vec{B}$ in toroidal coordinates. The magnetic field perturbation $\delta\vec{B}$ is chosen to model those generated by the ergodic divertor on Tore Supra, i.e. $\delta\vec{B}/B = \nabla\delta\psi \times \hat{e}_\varphi$, where the poloidal magnetic flux $\delta\psi$ is approximatively described by a sum over harmonics $\delta\psi = \sum_m \psi_m(r)\cos(m\theta - 6\varphi)$ and the poloidal spectrum $\psi_m(r)$ is modeled by $\psi_m(r) = \psi(r)\sin(\alpha_m)/\alpha_m$ with $\alpha_m = (m-18)\pi/6$. The safety factor $q(r)$ is monotonically increasing in the computational radial domain and the latter is restricted to the interval between the $q = 2$ and $q = 3$ surfaces. Slab geometry is used in the vicinity of a reference surface $r = r_0 = r_{q=2.5}$ and the radial profile of the perturbation $\psi(r)$ grows exponentially with radius reaching its maximal value ψ_{max} at $r = r_{q=3}$. It is then smoothly extrapolated to zero in a "buffer" zone $r_{q=3} < r \leq r_{q=3} + \Delta$. The operator $G \sim \nabla \times (\vec{B}/B^2) \cdot \nabla$ emerges from the toroidal curvature of the field lines. It appears in Eqs. (1) and (2) accounting for the compressibility of the diamagnetic and electric drift, respectively. The coefficient δ_c is essentially the ratio between a typical pressure gradient length and the major radius of the torus [12]. The coefficients ν, $\chi_\parallel$ and $\nu_\perp$ correspond to the perpendicular viscosity and the parallel and perpendicular heat diffusivity, respectively. The system is driven by a constant incoming flux that is given by the radial integral over the source S. The latter has Gaussian shape and is localized in a left "buffer" zone $r_{q=2} - \Delta \leq r < r_{q=2}$.

Eqs. (1), (2) describe the evolution of the complete fields of potential and pressure, i.e. the backreaction of the fluctuations on the profiles is included self-consistently [9]. Averaging over (unperturbed) magnetic surfaces, one obtains the evolution equations for the potential and pressure profiles, respectively. Using the relation between the potential and the $\vec{E} \times \vec{B}$ velocity, $(v_r, v_\theta) = (-\partial_{(r_0\theta)}\phi, \partial_r\phi)$, the equation for the potential can be directly written in terms of the poloidal velocity,

$$\partial_t \bar{v}_\theta = \ - \partial_r \left(\langle \tilde{v}_\theta \tilde{v}_r \rangle - \nu \partial_r \bar{v}_\theta \right) + A_{\delta B} \ , \tag{3}$$

$$\partial_t \bar{p} \ = \ - \partial_r \left(\langle \tilde{p} \tilde{v}_r \rangle - \chi_\perp \partial_r \bar{p} + \Gamma_{\delta B} \right) + S \ , \tag{4}$$

where $A_{\delta B} = -\langle \partial_{(r_0\theta)} \delta\psi \nabla_\parallel \phi \rangle$ and $\Gamma_{\delta B} = -\chi_\parallel \langle \partial_{(r_0\theta)} \delta\psi \nabla_\parallel p \rangle$ are respectively the flow generation and the heat flux due to the magnetic flutter. Note that the parallel gradient is $\nabla_\parallel = \nabla_{\parallel 0} + \{\delta\psi, \ \cdot \ \}$, where $\nabla_{\parallel 0}$ is the component due to the unperturbed field. Eq. (3)

shows that the generation of mean and zonal flows is governed by the balance between three different effects: the kinetic Reynolds stress, the viscous damping and the magnetic flutter. Equivalently, the total energy flux is decomposed into three components: the turbulent flux $\Gamma_{turb} = \langle \tilde{p}\tilde{v}_r \rangle$, the collisional damping $\Gamma_{coll} = -\chi_\perp \partial_r \bar{p}$ and the flux due to magnetic flutter $\Gamma_{\delta B}$. According to Eq. (4), in a statistically stationary state, the sum of the time average of these three fluxes must be equal to the radial integral of the source,

$$\int_0^T \frac{dt}{T} \left(\Gamma_{turb} + \Gamma_{coll} + \Gamma_{\delta B}\right) = \int_{r_{min}}^{r} dr' S(r') = \Gamma_{tot} = const \ ,$$

in the region $r \geq r_{q=2}$. Here, the following boundary conditions have been used: all fluctuations $\tilde{\phi}$, $\tilde{p}$, the mean potential $\bar{\phi}$ and the gradient of the pressure profile $\partial_r \bar{p}$ vanish at the left boundary of the computational box, $r_{min} = r_{q=2} - \Delta$. At the right boundary, $\tilde{\phi}$, $\tilde{p}$, $\bar{\phi}$ and $\bar{p}$ vanish.

Two different sets of simulations have been done, differing in the strength of the instability drive, characterized by the total incoming heat flux, $\Gamma_{tot} = 8$ and $\Gamma_{tot} = 36$, respectively. For both cases, one run has been performed with a maximal perturbation of the magnetic field of $\psi_{max} = 63.66$ which corresponds to a maximal value of the Chirikov overlapping parameter [1] of $\sigma_{Chir}^{max} = 3.0$. For comparison, a second simulation with $\psi_{max} = 0$ has been done in both cases. The values of the other parameters are kept constant for all four runs. They are given by $\nu = \chi_\perp = 2$, $\chi_\parallel = 1$, and $\delta_c = 0.04$. For a given series of toroidal wavenumbers, i.e. $n = 0, \Delta n, 2\Delta n, \ldots, n_{max}$, all Fourier modes that are resonant between $q = 2$ and $q = 3$ are included, i.e. those with poloidal wavenumbers m in the range $2n \leq m \leq 3n$ for each n. With $\Delta n = 2$ and $n_{max} = 40$, a total number of 441 Fourier modes is used. In the radial direction, 192 grid points are used. The perpendicular length scale is given by the resistive ballooning length [7] which is of the order of the ion Larmor radius at electron temperature. The normalized width of the radial interval is chosen as $r_{q=3} - r_{q=2} = 83.33$, and $\Delta = 25.53$. The normalized poloidal circumference at the reference surface is $2\pi r_0 = 2\pi \cdot 500$. The parallel length scale is the shear length which is of the order of the large radius and the normalized toroidal circumference is chosen as 2π. Time is normalized to the resistive interchange time [7].

3. Simulation Results and Discussion

Starting from initial conditions given by a rough estimate of the expected pressure profile and noise in all other components, the simulations are first run until a statistically stationary state is reached, i.e. the volume integrated pressure and velocity fluctuate around stationary mean values. The simulations are then continued for about 2000 normalized time units and the data analyzed. Both of the values chosen for the total incoming energy flux Γ_{tot} are such that the resulting mean pressure gradient is above the threshold for resistive ballooning instability. However, as one expects, the mean

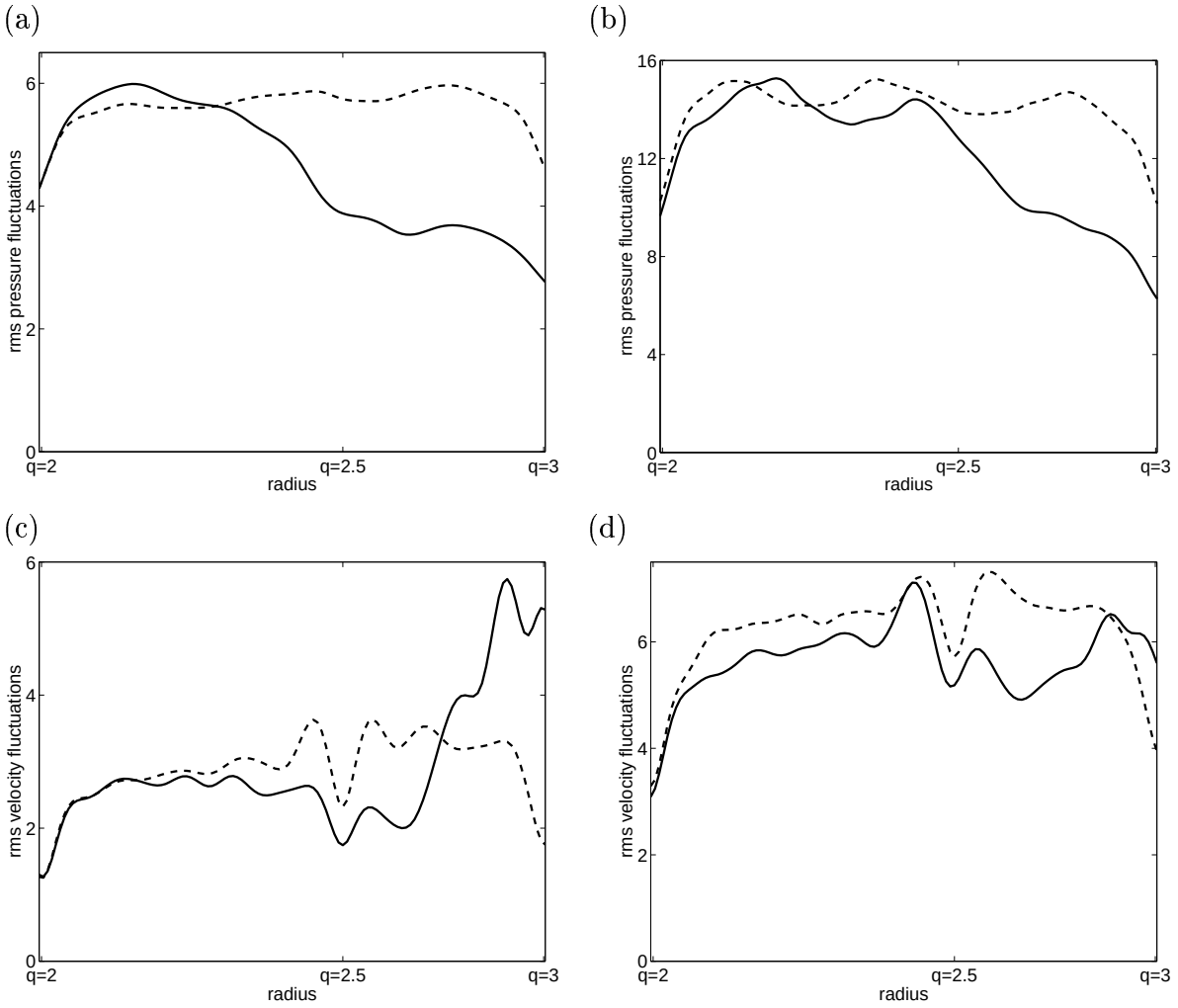

Figure 1. Time averaged radial profiles of the amplitudes of pressure and velocity fluctuations for $\Gamma_{tot} = 8$ (a,c) and $\Gamma_{tot} = 36$ (b,d). Full lines correspond to the case with magnetic perturbation and dashed lines indicate the reference case without magnetic perturbation.

pressure profile is closer to the threshold in the case $\Gamma_{tot} = 8$ compared to the case $\Gamma_{tot} = 36$.

Fig. 1 shows the radial profiles of the amplitudes of pressure and velocity fluctuations. In both cases, a clear reduction of the level of pressure fluctuations is observed in the region of stochastic magnetic field lines. Note that as the magnetic perturbation is maximal at $q = 3$ and decreasing exponentially radially inwards, the stochastic region is roughly localized between $q = 2.7$ and $q = 3$. Assuming that density fluctuations follow the behavior of pressure fluctuations, the decrease of their amplitude is in qualitative agreement with measurements on TEXT [2] and Tore Supra [3, 4, 5]. Concerning velocity fluctuations, the simulations show a completely different behavior from those of the pressure fluctuations. Close to the instability threshold ($\Gamma_{tot} = 8$), the level of velocity fluctuations is found to increase in the stochastic region

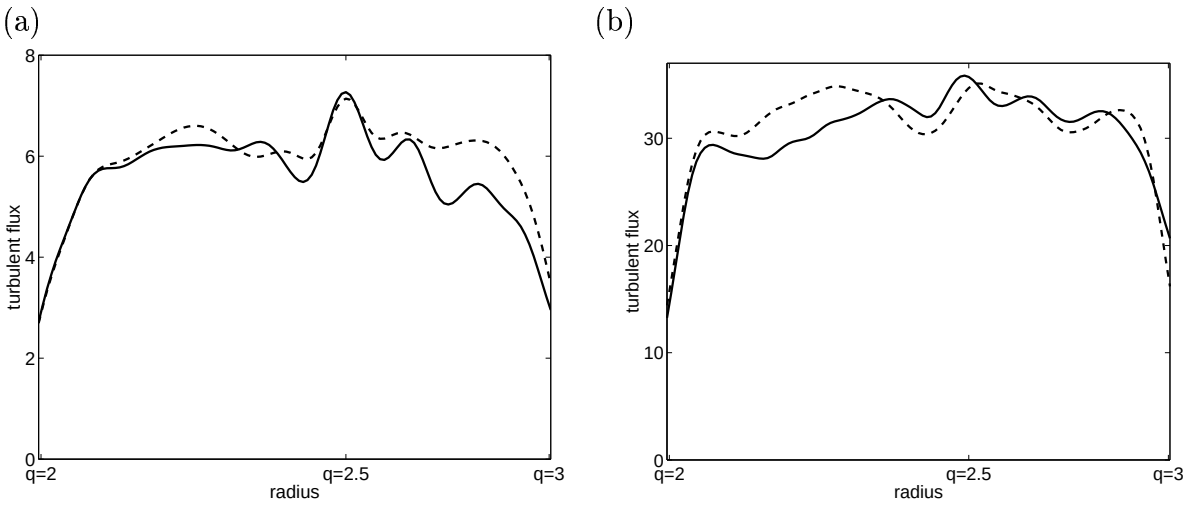

Figure 2. Time averaged radial profiles of the turbulent radial flux for $\Gamma_{tot} = 8$ (a) and $\Gamma_{tot} = 36$ (b). The cases with and without magnetic perturbation are indicated respectively by full and dashed lines.

and for the second case, it is roughly unchanged. This has an important consequence for the turbulent radial flux Γ_{turb} which is composed of the product of pressure and radial velocity fluctuations. As can be seen from Fig. 2, the time averaged level of this flux is roughly unchanged in the stochastic region, i.e. it *does not decrease* despite of a significant decrease of pressure fluctuations. This observation is in qualitative agreement with the analysis of heat deposition patterns on the plates of the ergodic divertor on Tore Supra. The latter shows that the turbulent heat diffusivity is of about the same order of magnitude compared to cases with limiter operation [1, 6]. Note that the phase between pressure and velocity fluctuations also enters into the determination of the turbulent flux.

From the poloidal wavenumber spectra (Fig. 3), it follows that the decrease of pressure fluctuations in the stochastic region is essentially due to a reduction of large scale structures. The small scales are unaffected. This is in qualitative agreement with measurements on Tore Supra [3, 4, 5]. Note that the "jump" in the spectrum at $m = 17, 18$ is difficult to interpret because the $(m, n) = (18, 6)$ component is in resonance with the most important component of the magnetic perturbation. The latter gives rise to nonzero equilibrium (i.e. time average) contributions in the resonant components of the pressure field, i.e. the pressure flattens on magnetic islands [7]. These contributions have to be subtracted from the complete field in order to get the pressure fluctuations. As the time average can only be calculated after the simulation has finished, the precision of this calculus is restricted by the relatively low number of time points (i.e. 3D fields) stored simultaneously (typically 100).

Again, the behavior of velocity fluctuations is different. As can be seen from Fig. 3, the increase of velocity fluctuations in the stochastic region (case $\Gamma_{tot} = 8$) is due to an increase of small scale structures. The picture is less clear in the second case but the

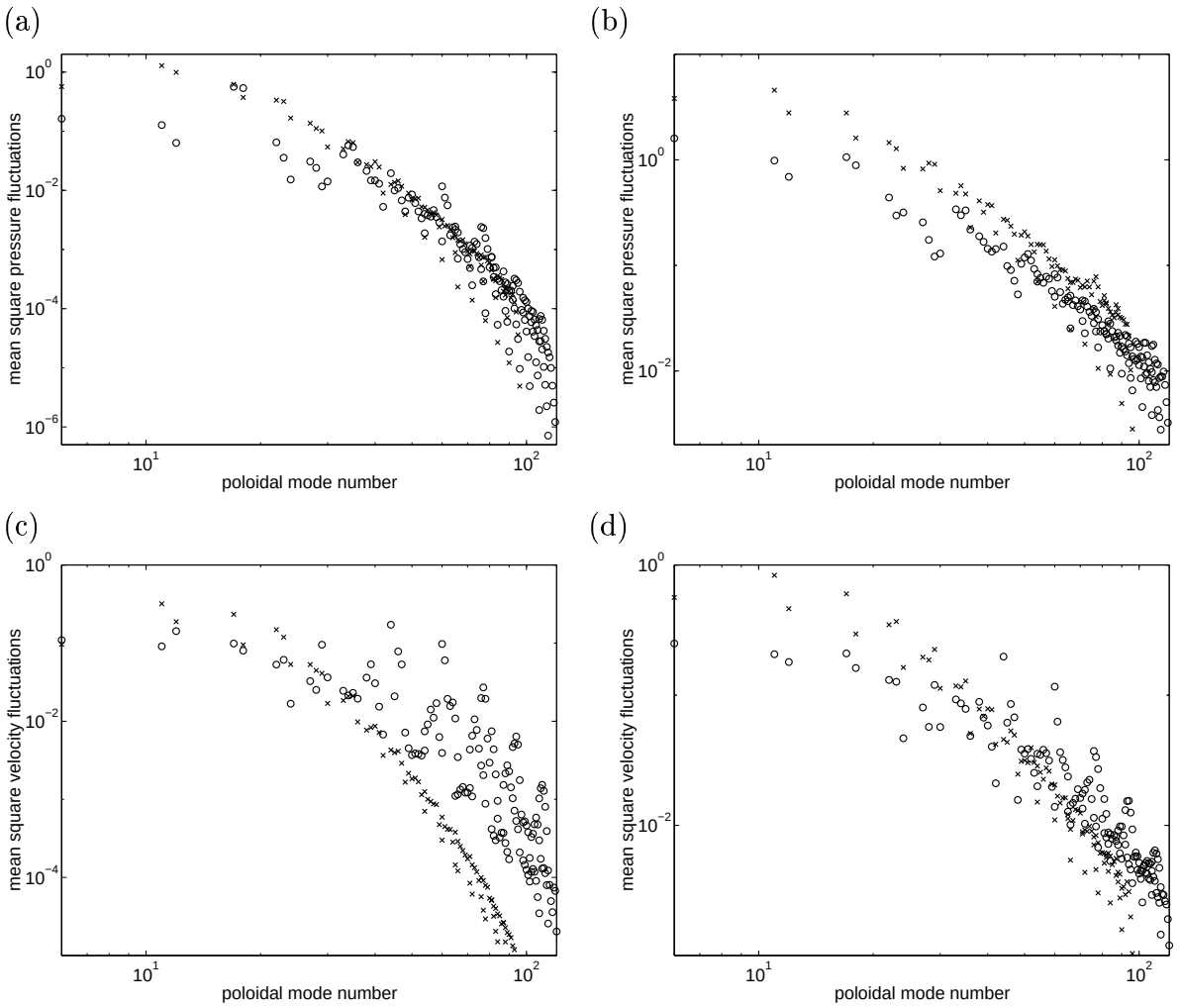

Figure 3. Time averaged poloidal wavenumber spectra of pressure and velocity fluctuations in the stochastic region for $\Gamma_{tot} = 8$ (a,c) and $\Gamma_{tot} = 36$ (b,d). Only those modes localized between $q = 2.7$ and $q = 3$ have been considered. Circles correspond to the case with magnetic perturbation and crosses indicate the reference case without magnetic perturbation.

tendency is the same.

The general results obtained from the wavenumber spectra are confirmed when looking at the frequency spectra of the fluctuations (Fig. 4): In the case close to the instability threshold one finds a reduction of low frequency pressure fluctuations and a significant increase of high frequency velocity fluctuations with a peak at $\omega \approx 0.3$. There is also a slight increase of high frequency pressure fluctuations, more precisely, a weakening of the slope of the spectrum is observed. The same result has been found in recent measurements on Tore Supra [5]. In the second case, the situation is less clear, although the tendency is the same for the velocity fluctuations. The peak in the frequency spectra, especially in the case close to the threshold, may be related to an eventually dominating linear mode. Note that such a mode must emerge from a solution

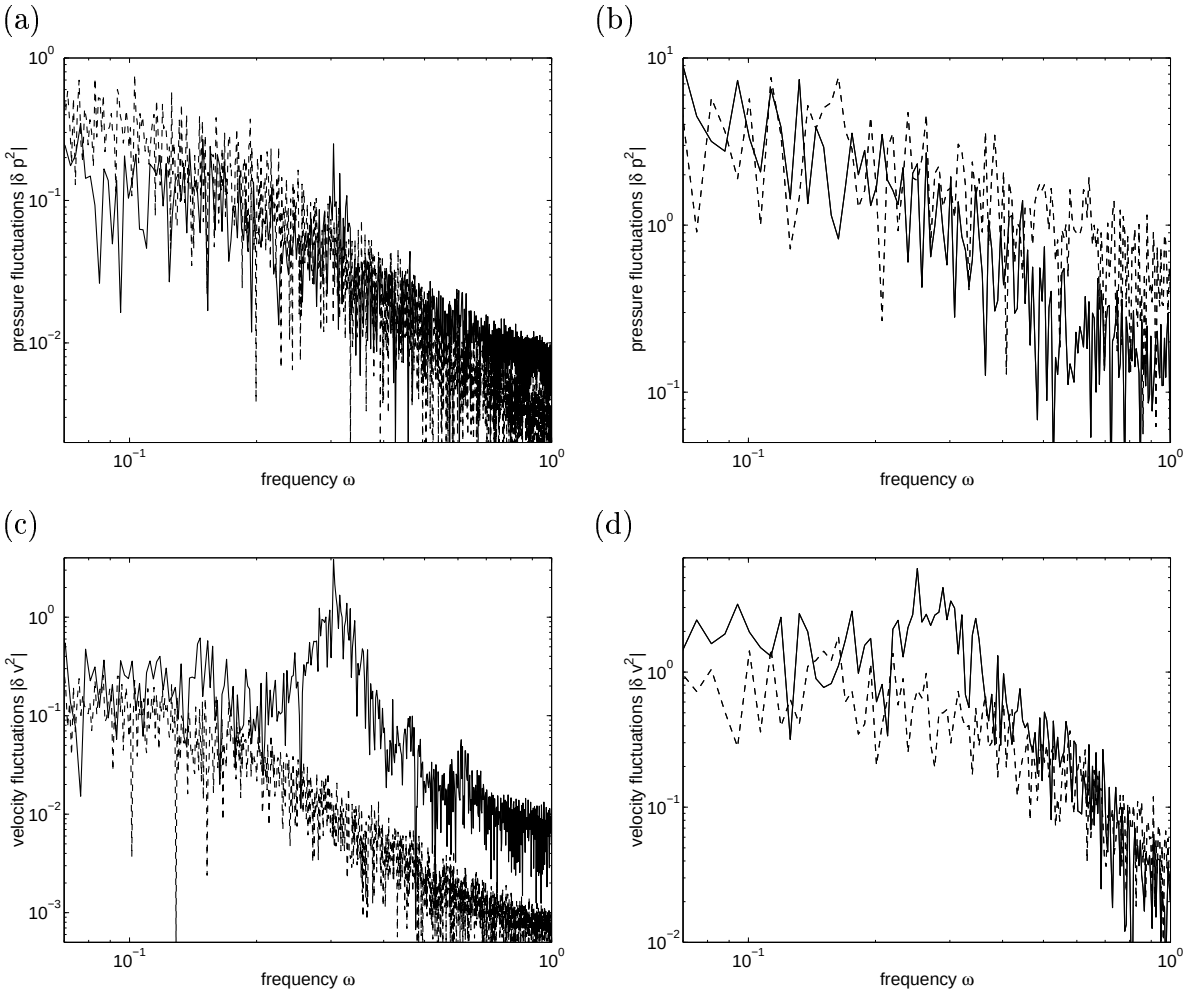

Figure 4. Frequency spectra of the (θ, φ) averaged pressure and velocity fluctuations at the radial position $r = r_{q=2.9}$ for $\Gamma_{tot} = 8$ (a,c) and $\Gamma_{tot} = 36$ (b,d). The cases with and without magnetic perturbation are indicated respectively by full and dashed lines.

of the *perturbed* linear problem, because unperturbed linear resistive ballooning modes do not have a real frequency.

Concerning the dynamics of the turbulent radial flux, it has been observed now in many different turbulence simulations [13, 14, 9, 15] that transport properties in tokamaks are governed by the interplay between radially extended convection cells (streamers) that give rise to large scale transport events and poloidal zonal flows that tend to self-regulate these bursts [10, 11]. Also experimental measurements show evidence of bursty transport [16, 17] and zonal flows [18]. Even if the time averaged mean value of the turbulent flux is roughly unchanged (as discussed before), the appearance of large scale transport events is expected to be strongly affected by the shearing of streamers due to the stochastic magnetic field. Additionally, the transport dynamics is modified by the influence of the magnetic field perturbation on the generation of mean and zonal flows (Eq. 3). As can be seen from Fig. 5, in both simulation cases, the mean

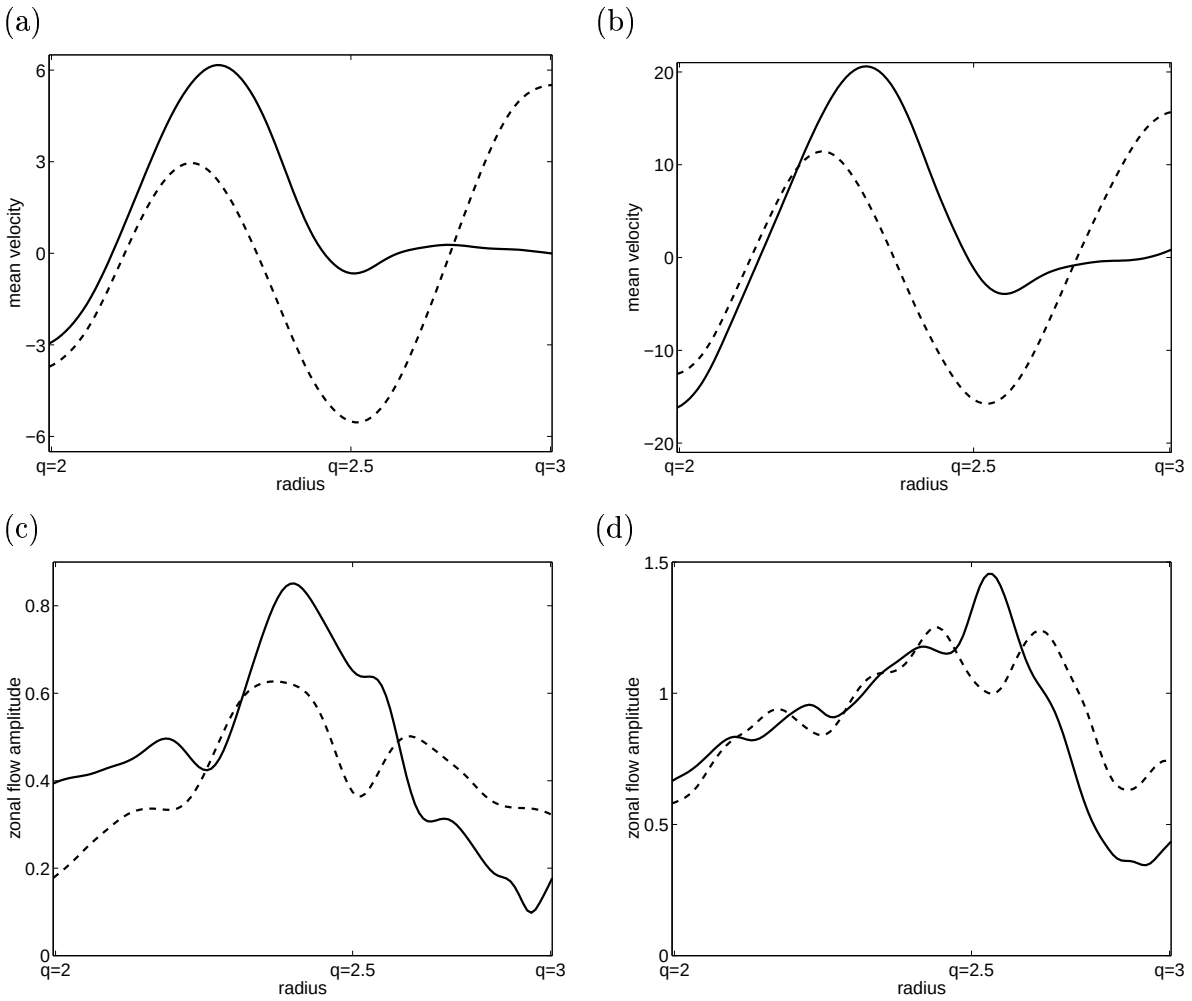

Figure 5. Radial profiles of the mean poloidal velocity and the time averaged amplitudes of zonal flows for $\Gamma_{tot} = 8$ (a,c) and $\Gamma_{tot} = 36$ (b,d). The cases with and without magnetic perturbation are indicated respectively by full and dashed lines.

flow is completely suppressed in the stochastic layer and the amplitude of zonal flows is reduced. The latter have been extracted from the total poloidal flow $\bar{v}_\theta$ by subtracting the low frequency (here $\omega < 0.07$) components.

In the more unstable case ($\Gamma_{tot} = 36$), the suppression of mean flow and reduction of zonal flows is found to be the dominant mechanism concerning the modification of the transport dynamics: The frequency spectrum of the turbulent flux is not very clear but roughly shows two different slopes for low and high frequencies, respectively, and the crossover between these two parts is shifted to low frequencies in the stochastic layer (Fig. 6b). This behavior is exactly the one observed when artificially suppressing the poloidal flow [9]. This means that large amplitude events (which are rare) can propagate in the stochastic region. We tried to illustrate this in Fig. 7, where the dynamics of the pressure profile is shown. Large scale transport events are high pressure bursts propagating radially outward or depressions traveling inward.

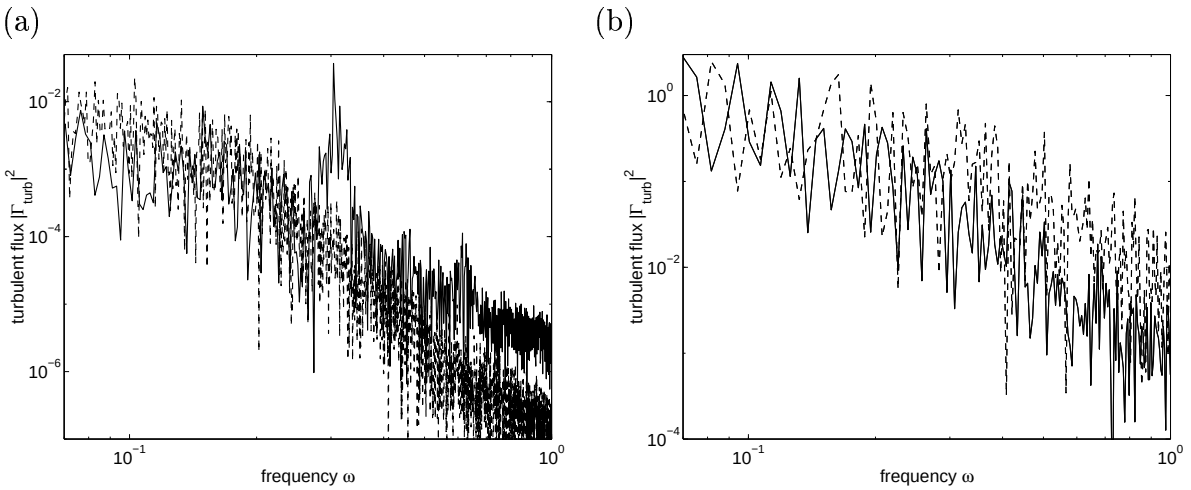

Figure 6. Frequency spectra of the turbulent radial flux at the radial position $r = r_{q=2.9}$ for $\Gamma_{tot} = 8$ (a) and $\Gamma_{tot} = 36$ (b). The cases with and without magnetic perturbation are indicated respectively by full and dashed lines.

The situation is different in the case close to the instability threshold. Here, although the mean and zonal flows are reduced, the spectrum of the turbulent flux shows a reduction of low frequency components and a weakening of the slope for high frequencies (Fig. 6a). Following the discussion above, this modification must be due to the second possible mechanism, i.e. a direct change of the fluctuations due to the magnetic field perturbation. This means that in the pressure profile dynamics fluctuations appear to be more rapid in the stochastic region and in general, the amplitudes of large events are reduced, i.e. crossing of these events is observed less frequently.

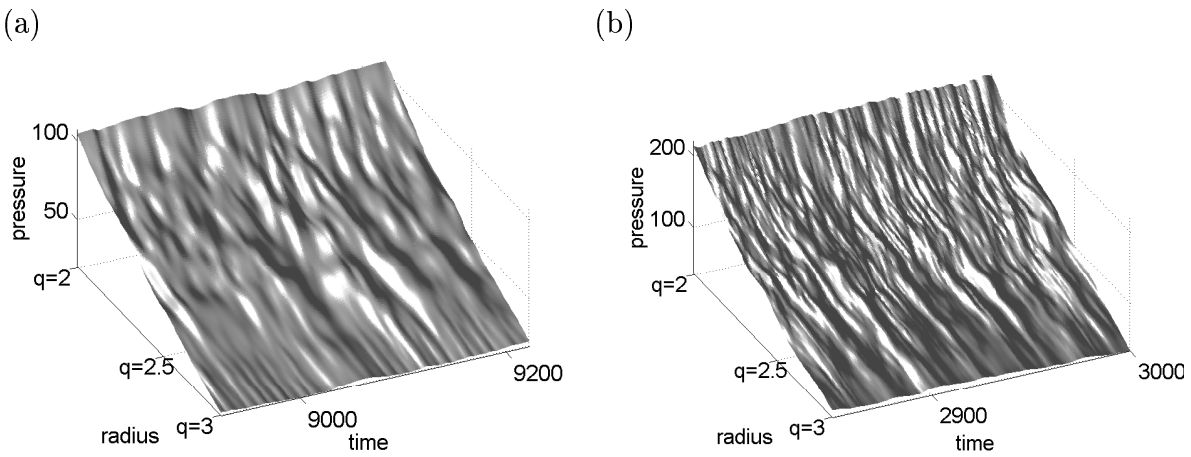

Figure 7. Time evolution of the radial pressure profiles for $\Gamma_{tot} = 8$ (a) and $\Gamma_{tot} = 36$ (b).

4. Conclusions

Perturbations of the equilibrium magnetic field with generation of stochastic magnetic field lines at the edge of a tokamak plasma have significant effects on turbulent fluctuations. Large scale pressure fluctuations decrease and small scale velocity fluctuations increase in the stochastic layer. This results in an roughly unchanged level of turbulent energy flux. For an ergodic divertor such as in Tore Supra this means that despite a lower level of pressure fluctuations, the turbulent cross-field transport is not quenched which is a beneficial effect for the performance of the divertor. Furthermore, applying this result to the issue of the onset of transport during ELMs where stochasticity is considered to play a significant role, one expects anomalous cross-field transport to remain effective in spreading the heat pulse.

Although the average value of the turbulent flux does not change significantly, its dynamics is strongly affected by the stochasticity of field lines. An important effect in this context is the suppression of mean poloidal flow and the reduction of zonal flows in the stochastic layer. This inhibits the self-regulation mechanism of large scale events, and therefore facilitates the existence of large bursts. For a high value of the incoming heat flux, this effect is dominant and large turbulent fronts propagating in the radial direction tend to resist the shearing induced by the stochasticity. For a case with lower turbulence drive, the amplitudes of large events decrease in the stochastic region and crossings appear less frequently.

Acknowledgments

Part of this work was done during the "Festival de Theorie", Self Organization and Transport in Electromagnetic Turbulence, Aix-en-Provence, France, 2001.

References

[1] Ghendrih P, Grosman A and Capes H 1996 *Plasma Phys. Control. Fusion* **38** 1653
[2] MacCool S C, Wootton A J, Aydemir *et al* 1989, *Nucl. Fusion* **29** 547
[3] Payan J, Garbet X, Chatenet J H *et al* 1995, *Nucl. Fusion* **35** 1357
[4] Devynck P, Antar G, Gunn J *et al* 2001 *J. Nucl. Mater.* in press
[5] Devynck P, Capes H, Gunn J *et al* 2001 submitted
[6] Grosman A, Ghendrih P, Capes H *et al* 1997 *Contrib. Plasma Physics*
[7] Beyer P, Garbet X and Ghendrih P 1998 *Phys. Plasmas* **5** 4271
[8] Beyer P, Sarazin Y, Garbet X *et al* 1999 *Plasma Phys. Control. Fusion* **41** A757
[9] Beyer P, Benkadda S, Garbet X *et al* 2000 *Phys. Rev. Lett* **85** 4892.
[10] Diamond P H *et al* 1998 *Proc. 17th IAEA Conf. Control. Fusion Plasma Phys. Yokohama, Japan*
[11] Lin Z *et al* 1999 *Phys. Rev. Lett.* **83** 3645
[12] Beyer P, Benkadda S, Bian N *et al* 2001 *Proc. 28th EPS Conf. Control. Fusion Plasma Phys.*
[13] Garbet X, Sarazin Y, Beyer P *et al* 1999 *Nucl. Fusion* **39** 2063
[14] Sarazin Y and Ghendrih P 1998 *Phys. Plasmas* **5** 4214
[15] Jenko F, Dorland W and Kotschenreuther M 2000 *Phys. Plasmas* **7** 1904
[16] Hidalgo C *et al* 1997 *Fusion Energy 1996 (Proc. 16th Int. Conf. Montreal, 1996), Vol. 1, IAEA, Vienna* 617

[17] Politzer P A 2000 *Phys. Rev. Lett.* **84** 1192
[18] Coda S, Porkolab M and Burell K H 2001 *Phys. Rev. Lett.* **86**, 4835